Spring 5-9-2018

# GEOCHEMISTRY OF SURFACE WATERS AND GROUNDWATER AT EKU'S MEADOWBROOK FARM, MADISON COUNTY, KENTUCKY

Reid E. Buskirk
*Eastern Kentucky University*, reid_buskirk1@mymail.eku.edu

# GEOCHEMISTRY OF SURFACE WATERS AND GROUNDWATER AT EKU'S MEADOWBROOK FARM, MADISON COUNTY, KENTUCKY

**By**

**REID EZEKIEL BUSKIRK**

**Submitted to Walter S. Borowski**

**Department of Geosciences**

**Eastern Kentucky University**

**Honors Thesis**

**May 2018**

# Introduction

Since the passage of environmental legislation in the late twentieth century, water contamination has mostly shifted from industrial point sources to urban and agricultural non-point sources. Agricultural activities often contaminate watersheds with excess nutrients (Dubrovsky et al., 2010). Excess nutrients in watersheds result in poor water quality and eutrophication—conditions sponsoring excess growth of algae—that also diminish dissolved oxygen concentration and decreases ecosystem diversity (Eby and Nelson, 2004). Eastern Kentucky University's (EKU) Meadowbrook Farm (Madison County, Kentucky), which raises both crops and livestock, is no exception (Fig. 1). Farm activities contribute dissolved nutrients (nitrate, $NO_3^-$; ammonium, $NH_4^+$; and phosphate, $PO_4^{3-}$) from fertilizers and animal waste into neighboring Muddy Creek via springs, runoff in tributaries, and subsurface drainage.

A joint research project was initiated by the EKU Departments of Agriculture, Chemistry, and Geosciences in the summer of 2016 to develop new methods to sequester phosphorous contamination on Meadowbrook Farm stemming from agricultural activities. Preliminary studies by Buskirk et al. (2017) and Evans et al. (2017) identified trends in nutrient contamination from the Farm. However, a more detailed understanding of the geochemical makeup of Farm surface waters, groundwaters, and their interactions is required to develop effective phosphorous sequestration methods in subsequent years of the project.

Groundwater and surface water contain dissolved ions from bedrock mineral dissolution, biological activity, anthropogenic activities, and contributions from natural sources. Different water sources possess differing geochemical, temporal, and transportation behaviors, which can be understood by studying suites of dissolved ions. Furthermore, Farm activities add dissolved ions in surface water and groundwater, changing their geochemistry.

### *Local Geology*

Most of the Farm upland area is underlain by the Devonian New Albany Shale (Fig. 2; Greene, 1968). Muddy Creek exposes the underlying Silurian Crab Orchard Formation which consists of claystone, shale, and dolomitic limestone (Green 1968). Most of the springs on the Farm property are sourced from the contact between the Boyle Dolomite and the underlying Crab Orchard Formation (Fig. 2).

### *Meadowbrook Farm*

EKU's Meadowbrook Farm is situated in eastern Madison County, Kentucky (Fig. 1). The Farm property is bound by Meadowbrook Road to the east and Muddy Creek to the south and west. The Farm is comprised of periodically rotated pastureland and cropland, and a central dairy complex (DC), consisting of milking facilities and barns. The Farm primarily raises dairy and beef cattle, soybeans, and corn. Previous studies on the Farm established sampling sites at springs, surface runoff, subsurface tile drains, surface runoff, Muddy Creek, the cow lagoon (CL), and the pig lagoon (PL) (Fig. 1; Buskirk et al. 2017; Evans et al. 2017).

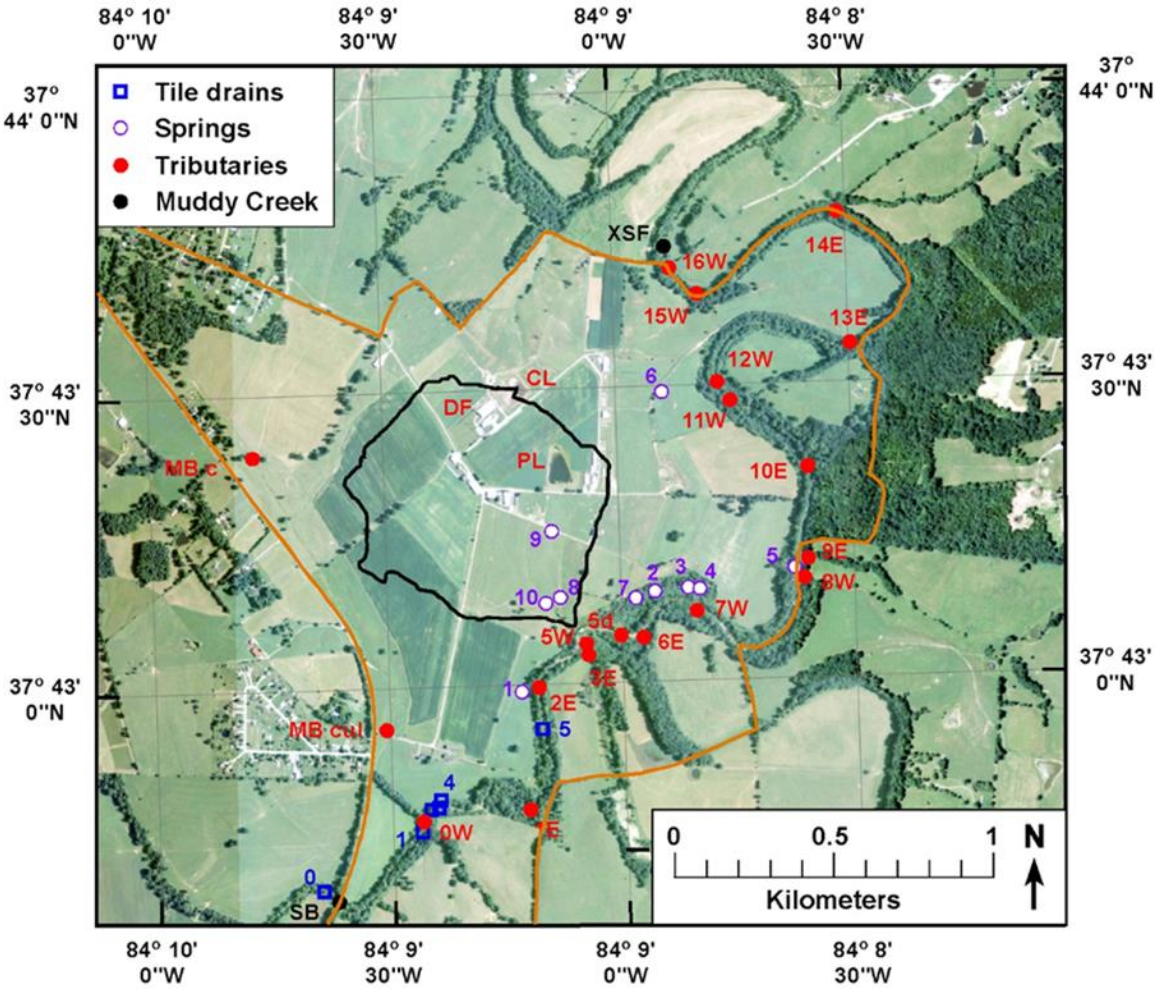


***Figure 1. Map of Meadowbrook Farm with labeled sampling sites. Springs, tributaries, tile drains, and Muddy Creek samples are labeled as white circles, red circles, blue squares, and black circles, respectively. The boundary of Meadowbrook Farm is show with an orange line. The black line outlines the sub-watershed of the Big Runoff Channel. The dairy complex (DF), cow lagoon (CL), and pig lagoon (PL) are also shown.***

Three general areas occur at the Farm (Fig. 1). The southern and western area of Meadowbrook Farm is drained by a runoff channel that flows south next to Meadowbrook Road and enters Muddy Creek at tributary 0W. The central area of Meadowbrook Farm contains a group of smaller runoff channels draining the central fields forming the Big Runoff Channel (BRC, Fig. 1). The BRC flows southeast and enters Muddy Creek at tributary 5W. The milking complex and pig sheds are situated on this sub-watershed. Manure effluent from the dairy barn is collected in the cow lagoon and the pig sheds leach waste into the pig lagoon. The northern area of Meadowbrook Farm consists of smaller tributaries entering Muddy Creek sourced from springs; spring 6 feeds tributary 11W, and springs 2 through 4 feeds tributary 7W. Several tributaries (11W, 12W, 15W, and 16W) drain the northern area of the farm. Westward flowing tributaries 1E, 2E, 3E, 6E,

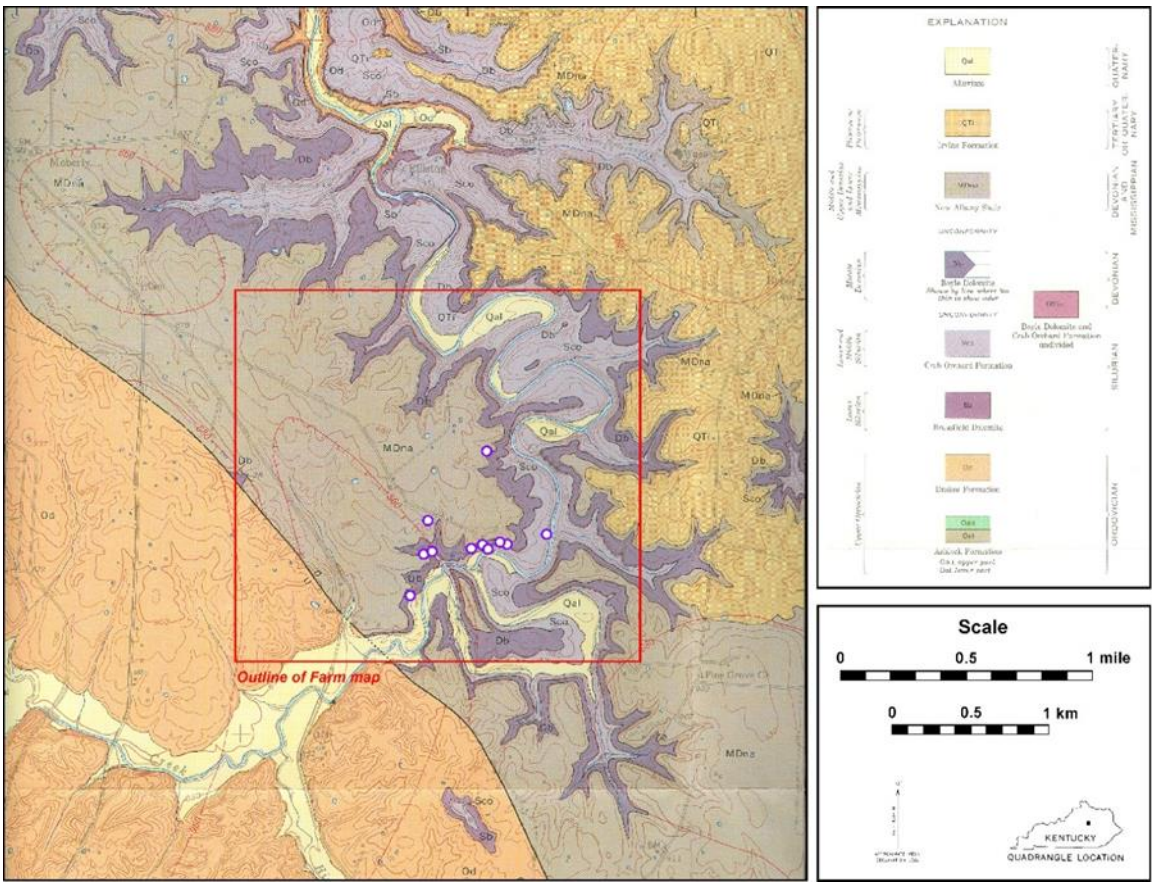


***Figure 1. Geologic map of a portion of the Moberly Quadrangle (Green 1968). Note springs rising out of the Boyle Dolomite as shown by the white circles. The red outline is that of the Meadowbrook Farm map shown in Figure 1.***

5E, 10E, 13E, and 14E drain into Muddy Creek from off-farm areas to the east of Muddy Creek.

Manure produced by dairy cattle is collected and dried for application to fields. The barn and dairy complex is cleaned periodically with the effluent being stored in the cow lagoon (Fig. 1) Water from the cow lagoon is also applied to crops. This is a potential source of nutrients and chemical species in watersheds, such as the BRC, which contains cornfields fertilized with manure.

### *Previous Studies*

Recent investigations by Buskirk et al. (2017) and Evans et al. (2017) have characterized $PO_4^{3-}$, $NO_3^-$, and $NH_4^+$ in surface waters and groundwater. $NO_3^-$ was the dominant nitrogen compound in Farm waters (Buskirk et al., 2017). Springs and the BRC were significant sources of nitrogen contamination, and to a lesser extent, $PO_4^{3-}$ (Buskirk et al., 2017; Evans et al., 2017). Surface waters experience increased dissolved nitrogen and decreased dissolved $PO_4^{3-}$ concentrations during wetter conditions (Buskirk et al., 2017; Evans et al., 2017). Springs were a significant source of dissolved $PO_4^{3-}$ and $NO_3^-$, and were higher than national values for agricultural groundwater reported by Dubrovsky

et al (2012) (Buskirk et al., 2017; Evans et al., 2017). In contrast, surface waters had lower dissolved $NO_3^-$, $NH_4^+$ and $PO_4^{3-}$ concentrations than national values (Buskirk et al., 2017; Evans et al., 2017).

Hydrograph separations were calculated by Kelley et al. (2017) to determine contribution of younger surface runoff and older groundwater in the total water volume discharged from the BRC watershed through a V-notch weir during summer storms in 2017. Three different storm types were observed. A groundwater dominated storm was observed on May 4-5, a surface water storm was observed on June 22-25, and an equally mixed groundwater and surface water storm was observed on August 4 (Kelley et al. 2017).

***Project Objectives***

By studying dissolved ions present in Farm surface and groundwater, previously observed nutrient trends can be placed into context to reveal insights into the behavior of groundwater and surface water on the Farm. Therefore, the current phase of the project aims to examine patterns of dissolved sodium ($Na^+$), calcium ($Ca^{2+}$), magnesium ($Mg^{2+}$), sulfate ($SO_4^{2-}$), bicarbonate ($HCO_3^-$), chloride ($Cl^-$), potassium ($K^+$), strontium ($Sr^{2+}$), bromide ($Br^-$), and fluoride ($F^-$), nitrate ($NO_3^-$), phosphate ($PO_4^{3-}$), and ammonium ($NH_4^+$). Other chemical parameters (pH, oxidation-reduction potential (ORP), specific conductivity (SC), percent dissolved oxygen (DO%), temperature, and alkalinity), local geology, and hydrological data (hydrographs and rainfall data) will also be used to characterize of the geochemistry, interpret interactions between different waters, and determine the transport mechanisms and behaviors of nutrients on the Farm.

Our project's primary objectives are: (1) a preliminary characterization the geochemistry of groundwater, surface water, soil water, the pig lagoon, the cow lagoon, and Muddy Creek; (2) identify end member water type compositions and determine any mixing of water types; (3) and to temporally analyze the changes in water chemistry during rainstorm events to discern hydrological changes in the BRC and to determine hydrological pathways for nutrients.

# Methodology

### *Hydrological Data*

BRC discharge was quantified using a V-notch weir constructed near station 5W. The weir is fitted with a pressure transducer which measures the water depth of the pool immediately behind the weir using the pressure exerted by the water column and the atmosphere. Water depth is proportional to discharge over the weir so a dynamic record of discharge from the BRC is recorded (Fig. 3). Precipitation levels were monitored by weather station ELST located on the Farm property and operated by the Kentucky Mesonet (www.mesonet.org; Fig. 4).

### *Sampling Strategy*

To determine dissolved ion concentrations and other chemical parameters in different Farm water types, sampling stations were established on the Farm and along Muddy Creek (Fig. 1, Buskirk et al., 2017, Table A1). A list of the sampling stations (Table A1) and the corresponding GPS coordinates (Table A1) are included in the Appendix. Fifty-six surface water sampling stations occur in tributaries draining Meadowbrook Farm, Muddy Creek and off-farm areas to the east. These sampling stations are used to ascertain how Farm water chemistry changes in runoff and in Muddy Creek. Sampling stations at eleven springs and at seven tile drains were established to

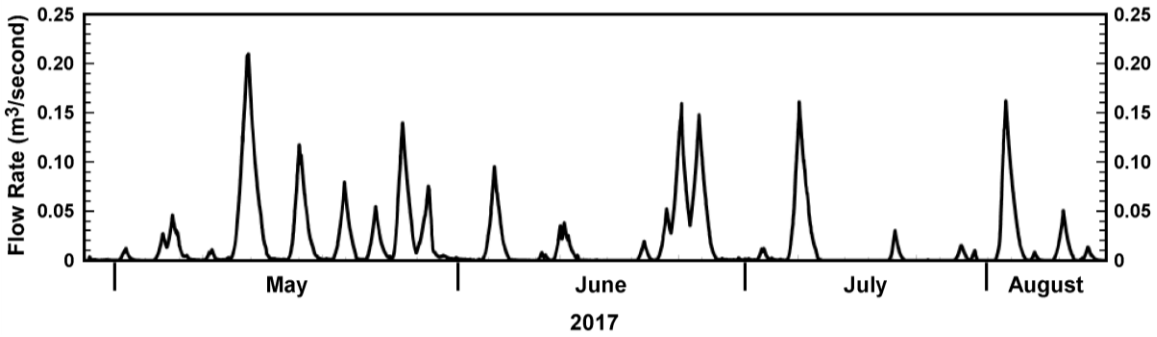


***Figure 2. Discharge hydrograph through the weir during the 2017 field season (Kelley, 2017).***

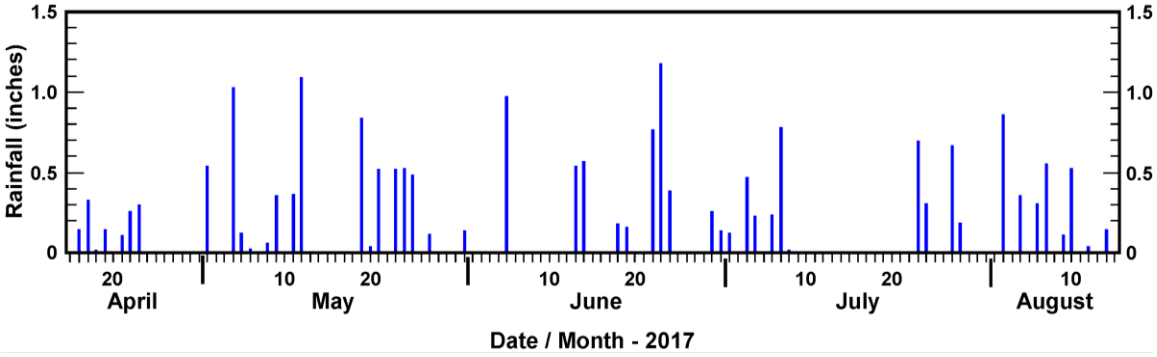


***Figure 3. Precipitation at Meadowbrook Farm (station ELST, Kentucky Mesonet) during the 2017 field season (www.mesonet.org).***

sample groundwater and soil, respectively. Water samples were also collected from the cow and pig lagoons to determine their geochemistry. Storm water samples were collected at the weir from the BRC watershed to understand how water chemistry evolved during rainfall and runoff events.

### *Sampling & Techniques*

In 2017, water samples were collected on thirteen different sampling days under a variety of different rainfall conditions (Table 1). Water samples were collected in 60-ml syringes and passed through a 0.45 μm filter. Samples destined for nutrient analysis were acidified to a pH of ~2 with concentrated $H_2SO_4$; and samples destined for anion and cation analysis were collected without acidification. Both acidified and unacidified samples were stored in 20-ml borosilicate vials and refrigerated until laboratory analysis, which typically occurred one to two days after sampling (Borowski et al. 2012; Clesceri et al. 2012). Sample duplicates and triplicates were collected to test the variation of field samples.

### *Nutrients Measurements*

We measured dissolved $NO_3^-$, $NH_4^+$, $PO_4^{3-}$ via colorimetric spectrophotometry. To quantify $NO_3^-$, the cadmium reduction method was used (Hach, 1986), which measures both dissolved nitrate ($NO_3^-$) and nitrite ($NO_2^-$) but $NO_3^-$ is the predominant component (Eaton et al., 2005). Standards with concentrations of 0.0 to 12.6 mg/L N-$NO_3^-$ were made for $NO_3^-$.

To measure $NH_4^+$, the sodium hypochlorate method established by Solorzano (1969) and as modified by Gieskes et al. (1991), was used. The sodium hypochlorate method measures both dissolved ammonium ($NH_4^+$), and ammonia ($NH_3$), but $NH_4^+$ is the predominant compound. Standards with concentrations of 0.0 to 12.7 mg/L N-$NH_4^+$ were made for $NH_4^+$.

To measure $PO_4^{3-}$, the ascorbic acid method was used (Strickland and Parsons, 1986; Eaton et al., 2005) as modified by Gieskes et al. (1991). Standards with concentrations of 0.0 to 5.3 mg/L P-$PO_4^{3-}$ were made for $PO_4^{3-}$.

To calculate nutrient concentrations, the standard solutions were used to construct linear calibration curves via least squares regression. Correlation coefficients ($r^2$) values ranged from 0.9844 to 1.000; typical standard curves and calculated nutrient concentrations are presented in the appendix (Figs. A2; Table A3) These methods have a precision of ± 0.1 mg/L, and measurements were calibrated to an external standard.

**Table 1. Sampling during the field season of 2017.**

| Storm Sampling | Baseline Sampling |
|---|---|
| May 4-5, 2017 | May 16, 2017 |
| June 4-5, 2017 | May 31, 2017 |
| June 13-14, 2017 | June 20, 2017 |
| June 22-25, 2017 | July 6, 2017 |
| July 6-7, 2017 | July 21, 2017 |
| August 4, 2017 | July 26, 2017 |
| - | August 4, 2017 |

***Anion and Cation Measurements:***

Inductively coupled plasma optical emission spectrophotometry (ICP-OES) was used to measure $Ca^{2+}$, $Mg^{2+}$, $K^{+}$ $Na^{+}$, $Sr^{2+}$, and $Fe^{3+}$ in the water samples for the Cindy event and for baseline surface water and groundwater samples by ACT Labs (Actlabs, 2017).

Ion exchange chromatography with a Metrohm 930 Compact IC Flex was used to quantify $F^{-}$, $Cl^{-}$, $Br^{-}$, $NO_3^{-}$, $PO_4^{3-}$, and $SO_4^{2-}$ concentrations in unacidified water samples. Linear calibration plots of each cation and anion were constructed, and $r^2$ values ranged from 0.9972 to 1.000. Example calibration plots are presented in the Appendix (Table A5, Figs. A4). Method blanks of 18.2 MΩ deionized water and $NaHCO_3/Na_2CO_3$ eluent were used to confirm laboratory cleanliness of the matrix. Matrix spikes were conducted for each analyte to determine any matrix effect. Measurements were calibrated to an external standard. Duplicates were analyzed, and measurement uncertainty was found to be less than 10% for most analytes. Table A6 presents the percent difference for our analytes.

***Alkalinity and Probe Measurements of General Chemical Parameters.***

LabQuest 2 Probestation equipment and a YSI field probe were used to determine the pH, ORP, SC, DO%, and temperature of the water samples in the field or within 1-2 days of collection. Alkalinity was determined via the bromocresol green-methyl red autotitration method (Hach, 1986), typically 1-2 days after collection. Since pH of water samples were almost entirely neutral to mildly basic, alkalinity is assumed to be essentially equal to the concentration of $HCO_3^{-}$ in water samples (Fig. 5).

# Results & Discussion

***General Chemical Parameters:***

Specific conductivity (SC) was higher in springs than surface water or storm water, while storm water had a higher SC than surface waters. High SC in springs is likely due to dissolution of local bedrock and other solutes. Low SC in surface waters suggest sorption of cations, complexation, and/or biological uptake of nutrients. Storm waters had a larger range of SC, which shows pulses of dissolved solute transport, especially during rain events.

Percent dissolved oxygen was generally approaching or exceeding 100% saturation for samples from all water types. This suggests groundwater is fairly young since the bacteria have not had enough time to consume oxygen to generate values approaching through decomposition. Also, storm waters exhibit a tight percent dissolved oxygen range (~70-80% saturation), which indicates large amounts of oxygen are incorporated in rainfall.

Predominantly positive ORP values indicate all Farm water types are oxidizing. This is likely due to high concentrations of oxidizing species, especially dissolved oxygen and $HCO_3^-$, which is readily absorbed from bedrock and is the dominant anion in waters. Surface, spring, and storm waters exhibit the lowest, mid-range, and highest ORP values, respectively. High ORP within storm waters is likely due to increased dissolved oxygen from precipitation and runoff. Spring ORP is likely sourced from bedrock dissolution of $HCO_3^-$ and dissolved oxygen. Lower ORP in surface water may be due to of volatilization of dissolved oxygen as temperatures increase, consumption by biological activity, and buffering of $HCO_3^-$ with compounds released from organic material.

All water types have neutral to mildly basic pH which indicates local $CaCO_3$ bedrock dissolution controls the pH of surface and spring waters. The pH of storm waters is similar to the pH of surface and groundwater, likely due to the slightly acidic pH of normal rainwater and buffering by $HCO_3^-$ from baseflow groundwater. Temperature of spring water was generally lower than surface waters which demonstrates that groundwater increases in temperature as it flows overland from springs due to interactions with the surrounding atmosphere. The range of the six temperature points from storm samples are within the ranges of both groundwater and surface water, suggesting the mixing of these two water types.

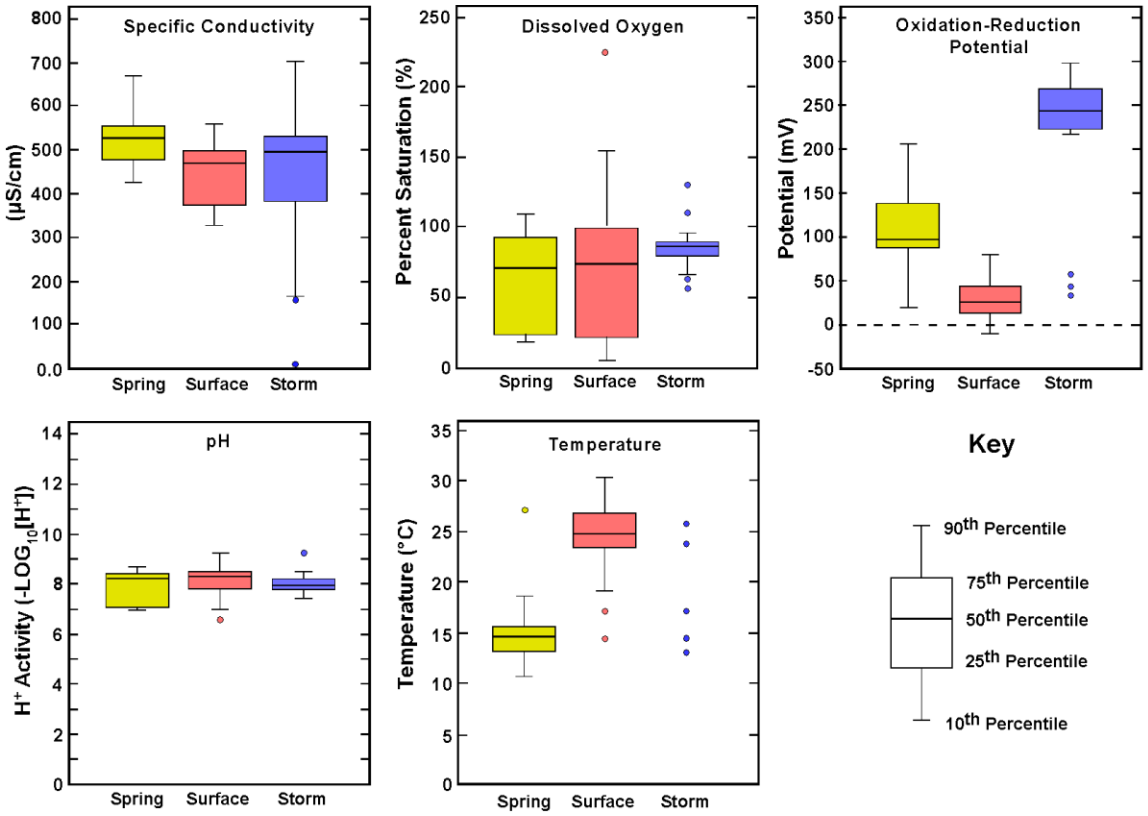


***Figure 4. Box and whisker plots of specific conductivity (SC), dissolved oxygen (%), oxidation-reduction potential (ORP), temperature, and pH.***

### *Major Cation & Anion Chemistry of Selected Source Waters:*

Overall, $HCO_3^-$ is the dominant anion species, and $Ca^{2+}$ and $Mg^{2+}$ are the dominant cation species in Farm waters (Fig. 6). High $HCO_3^-$ concentrations cause Farm waters to have neutral to slightly basic pH due to buffering. This reflects dissolution of local dolomite ($CaMgCO_3$) bedrock (Green, 1968) with local groundwater and surface water. Furthermore, this suggests Farm water chemistry is controlled by groundwater baseflow from springs (Greene, 1968). $HCO_3^-$ outliers are predominantly sourced from a $HCO_3^-$-enriched storm, which occurred on June 13-14 (Fig. 6). $Ca^{2+}$ concentrations are greater than $Mg^{2+}$, which reflects the larger solubility and preferential dissolution of $Ca^{2+}$ over $Mg^{2+}$ from bedrock. Low concentration $Ca^{2+}$ outliers reflect baseflow dilution during the surface water dominated June 22-25 storm, tropical storm Cindy.

The cow lagoon contains the largest chloride and sulfate concentrations compared to the rest of Farm and occur as outliers in Figure 6 (Fig. 7). Chloride and sulfate become concentrated in the cow lagoon during cycles of evaporation and refilling from the milking barn. The manure from this pond is administered as fertilizer on the Farm and is therefore the likely source of $Cl^-$ and $SO_4^{2-}$ in Farm waters. We have no evidence of direct leakage from the cow lagoon.

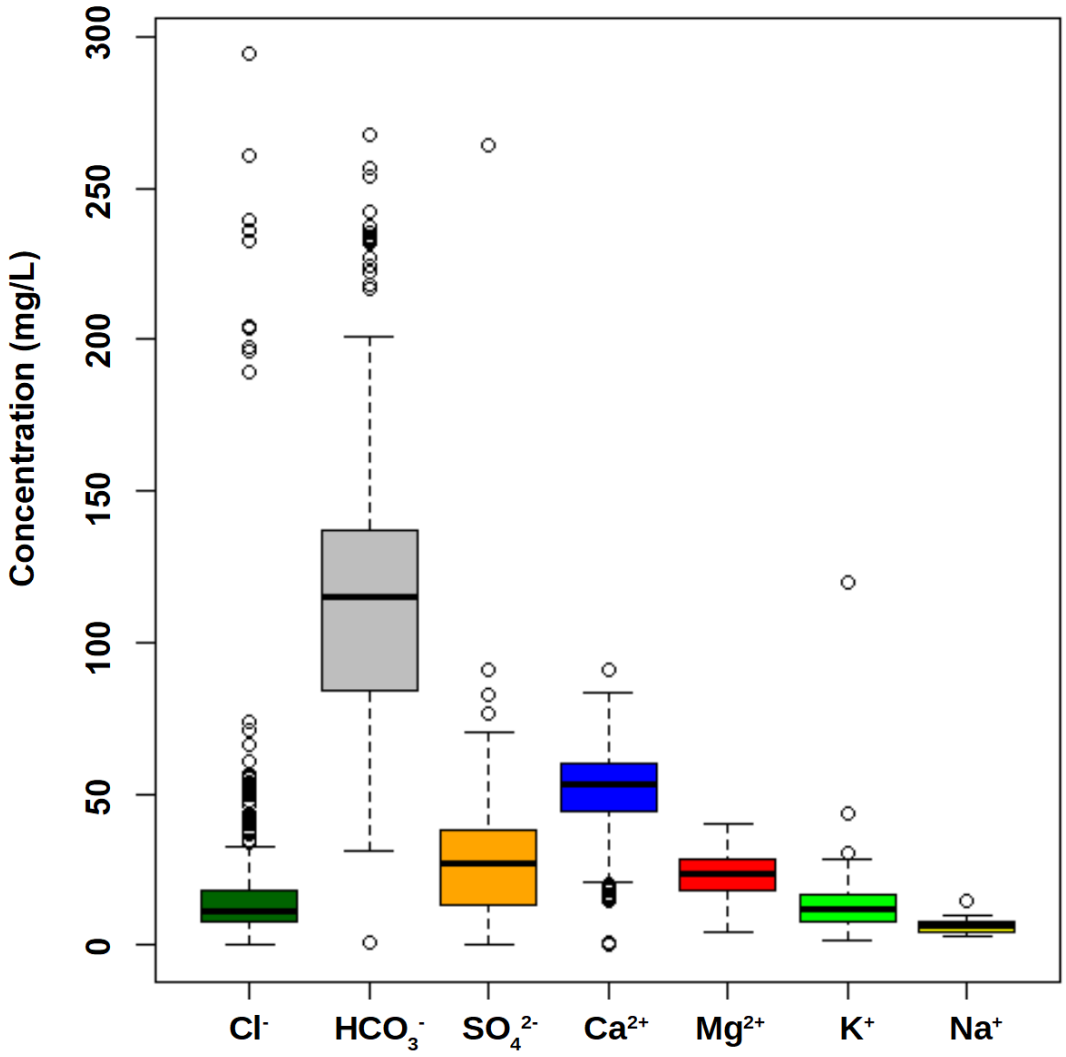


***Figure 6. Box and whisker plots of chloride ($Cl^-$), bicarbonate ($HCO_3^-$), sulfate ($SO_4^{2-}$), calcium ($Ca^{2+}$), magnesium ($Mg^{2+}$), potassium ($K^+$), and sodium ($Na^+$) in Farm waters. The key to the box and whisker plots is presented in Figure 5. Values outside of the 10th and 90th percentiles are shown as open circles.***

$Na^+$ and $K^+$ concentrations are comparable to $Cl^-$ and $SO_4^{2-}$, which suggests they are sourced from the Cow Lagoon via manure application (Fig. 6). However, cation analysis of the cow lagoon has not been conducted to verify this hypothesis. It is also likely that $K^+$ and $Na^+$ are sourced from Farm soils since both exhibit relatively uniform concentrations in spring, soil, and surface waters (Fig. 8).

Median values of chloride vary little in the BRC, other tributaries, groundwater, and storm runoff (Fig. 9). High $Cl^-$ concentrations in groundwater are perhaps due to concentration of $Cl^-$ from evapotranspiration during infiltration or accumulation in karst conduits. Many tributaries on the Farm, including the BRC, have baseflow sourced directly from groundwater springs, which coupled with manure application and fertilizers, likely result in high $Cl^-$ concentrations for Farm tributaries. Higher $Cl^-$

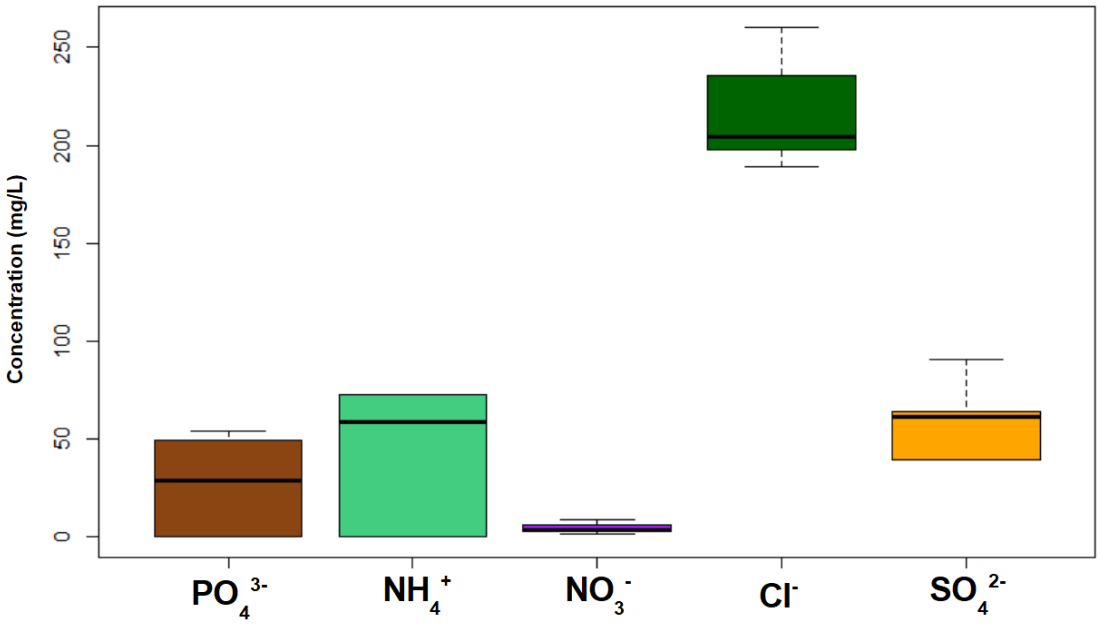


***Figure 7. Box* and whisker plots (see key, Fig. 5) of phosphate, ammonium, nitrate, chloride, and sulfate concentrations in the Cow Lagoon (CL) (Fig. 1).**

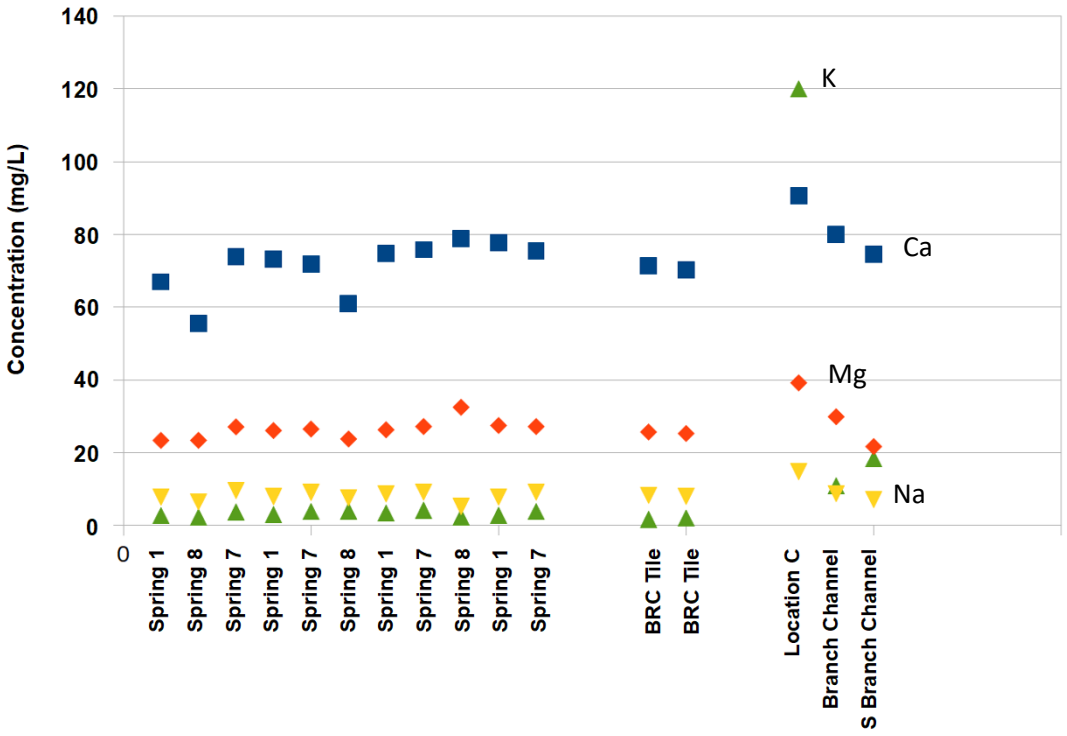


***Figure 8. Variation of sodium (yellow triangles), potassium (green triangles), magnesium (red diamonds), and calcium (blue squares) concentrations in spring, tile, and surface waters.***

concentrations in tributaries outside of the BRC may be due to manure applications and road salting in other areas of the Farm. Storms also are expected to have higher $Cl^-$ concentrations since these events would flush Cl from the Farm surface and possibly from karst conduits. Soil water exhibits slightly lower $Cl^-$ concentrations than surface water, which suggests chloride is transported overland in surface waters and storm waters. Muddy Creek and the Pig lagoon exhibit the lowest concentrations of Cl on the Farm. The PL is not significantly contaminated by agricultural activity. Therefore, $Cl^-$ is seems sourced from precipitation, concentrated in cycles of evaporation in the Pig Lagoon. Muddy Creek exhibits low $Cl^-$ concentrations, which suggests that the Farm does not significantly contribute chloride during baseflow conditions.

Sulfate concentrations are generally higher than chloride concentrations, with median values ranging from 1.6 to 32.1 mg/L (Figs. 9-10). Sulfate exhibits the lowest concentrations in the Pig Lagoon, as the water body is relatively unaffected by agricultural activities (Fig. 10). Muddy Creek exhibits the second lowest $SO_4^{2-}$, perhaps suggesting that collective $SO_4^{2-}$ contamination from the Farm and upstream farms increase proportionally to $SO_4^{2-}$ concentrations in Muddy Creek. Tributaries, the BRC, tiles, and groundwater exhibit similar median sulfate concentrations (Fig. 6, 10). This suggests SO42- is sourced from cow manure applications and enters surface, soil, and groundwater. This also suggests rapid infiltration of $SO_4^{2-}$ into local soil water and groundwater. Storm waters exhibit the highest median $SO_4^{2-}$ concentrations, which suggests increased $SO_4^{2-}$ transport from the BRC. Minor amounts of $SO_4^{2-}$ are possibly contributed from source bedrock as well.

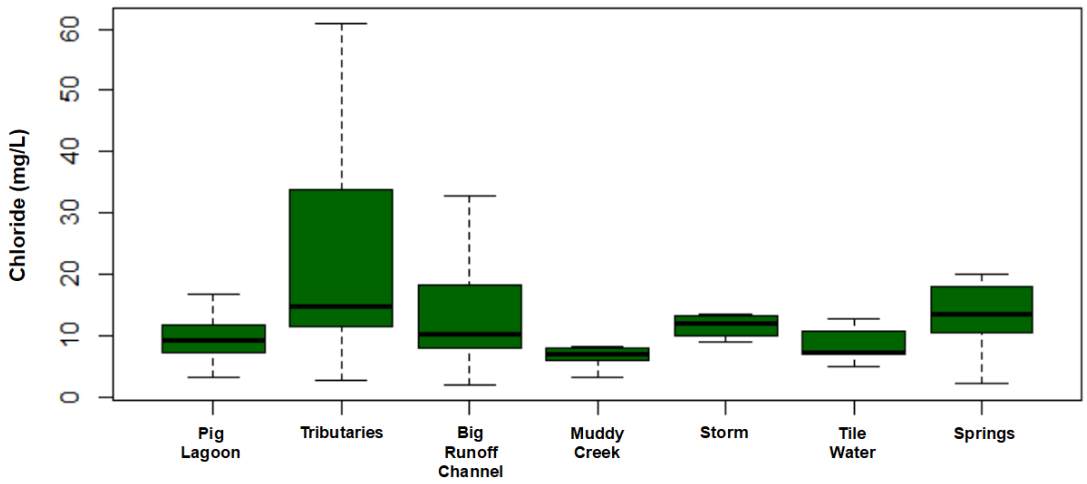


*Figure 9. Box and whisker plots of dissolved chloride concentrations of different hydrological systems and water types on the Farm. See Figure 5 for the key.*

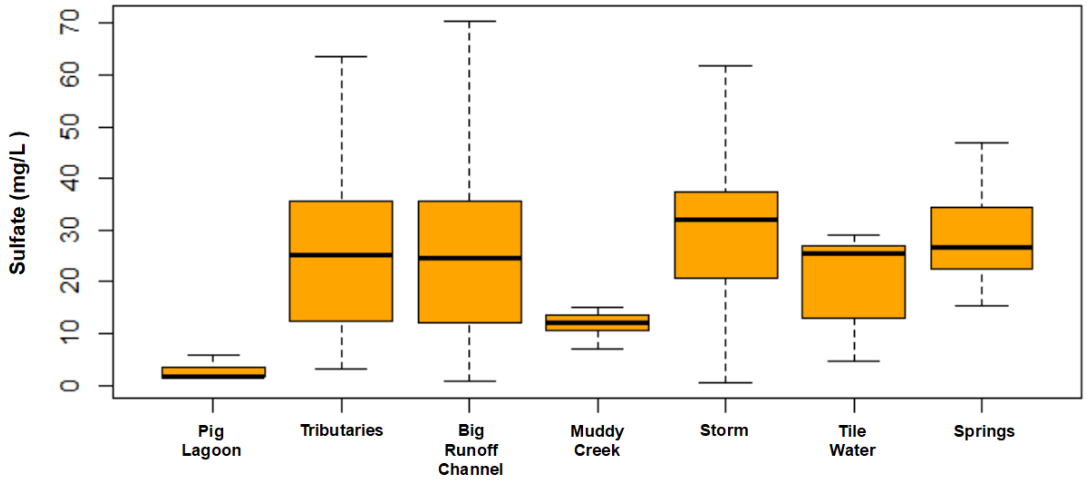


*Figure 10. Box and whisker plots of dissolved sulfate concentrations of different hydrological systems and water types on the Farm. See Figure 5 for the key.*

***Trace Element & Heavy Metal Trends:***

Overall, Farm waters exhibit very low concentrations of trace elements and heavy metals such as Ag, As, Bi, Cd, Ce, Pb, Se, Sn, Te, Ti, U, V, and Y. However, trace amounts of Ba, Mo, Sb, Sr, Tl, and Zn were detected. Ba and Mo, are likely sourced from Farm activities since higher concentrations (50-1170 µg/L Ba and 12 µg/L Mo) occur in the BRC. Sr and some Ba are sourced from local bedrock. Ba, Sr, and Ca have similar size to charge ratios (Chang and Goldsby, 2014, p. 260), which permits substitution of Sr and Ba for Ca in the dolomite crystal lattice. Mo, Sb, and Tl sporadically exhibit trace concentrations (<12 µg/L) and should not be a significant concern for water quantity. Zn is likely sourced from metal alloys in piping, equipment, building materials, fencing, fence posts, and other metal objects on the Farm.

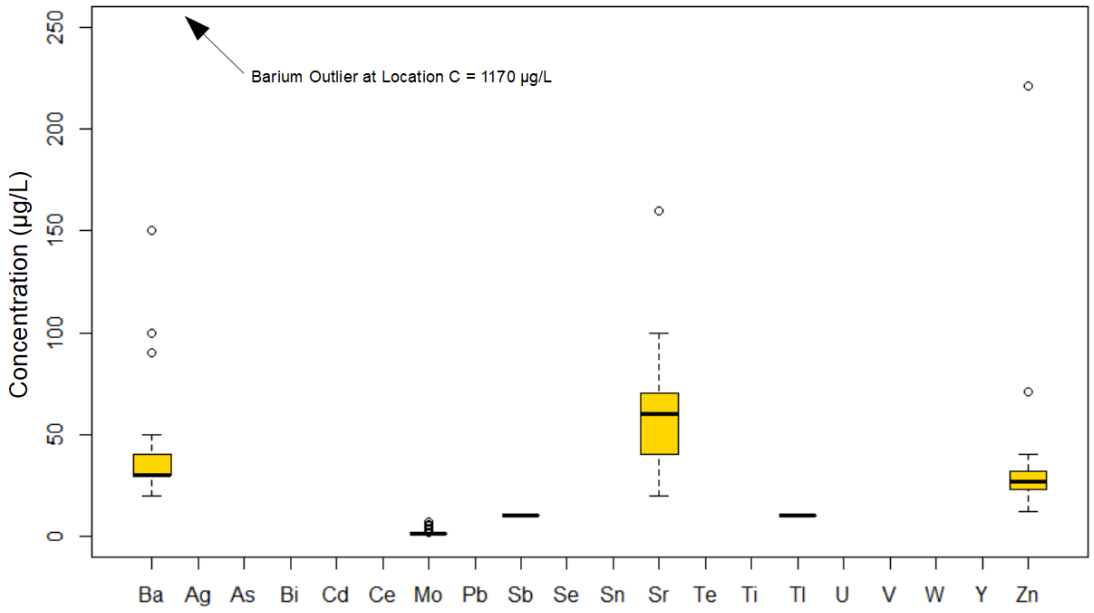


***Figure 11. Box* and whisker plots of dissolved trace metal concentrations in Farm waters. See Figure 5 for the key.**

***Overall Nitrate Trends:***

All surface water types exhibit lower $NO_3^-$ concentrations than the national surface water values, including storm waters (Fig. 12; Dubrovsky et al., 2010). Most elevated $NO_3^-$ concentrations in the BRC and other areas of the Farm are likely from manure application (Fig. 7). The pig lagoon exhibits the lowest $NO_3^-$ concentrations on the Farm, which is likely due to minimal contamination from agricultural activities, except for effluent leaching from the pig sheds. Therefore, the Pig Lagoon provides an example of relatively uncontaminated end member of Farm waters. The BRC generally contains relatively low $NO_3^-$ concentrations compared to source springs, suggesting nitrogen degassing or uptake by organisms (Fig. 12).

Nitrate enrichment has been observed in groundwater in previous studies and during the summer of 2017 (Buskirk et al., 2017). The concentrations measured in 2017 were lower than national values. This contrasts with the results of previous studies, which found groundwater $NO_3^-$ to be larger than the national values (Buskirk et al., 2017). This shows annual variability in $NO_3^-$ concentrations in groundwater, and suggests relatively short residence times for groundwater. Different $NO_3^-$ concentrations in groundwater can be expected between years due to different rainfall patterns. The summer of 2017 was unusually wet and exhibited several storm events, with relatively little drought (Figs. 3, 4). This likely flushed Farm groundwater and karst conduits more frequently, reducing $NO_3^-$ buildup.

However, these different values may also be due to the different sample locations explored during the present and previous studies. The contemporary project focused almost exclusively on springs 1, 7, and 8. Previous sampling showed that springs 2 and 4 consistently exhibit high nitrate values (Buskirk et al., 2017). Not including springs 2 and 4 in 2017 sampling may have skewed the dataset towards lower concentrations.

Future research on the Farm should consider sampling of all groundwater springs, since $NO_3^-$ concentrations vary significantly between springs (Buskirk et al., 2017). For the purpose of this study however, focusing on springs 1, 7, and 8 is reasonable since we aim to use the BRC as a representative watershed. However, future studies may consider investigating the chemical variation of subwatersheds on the Farm to understand the impact of different agricultural activities.

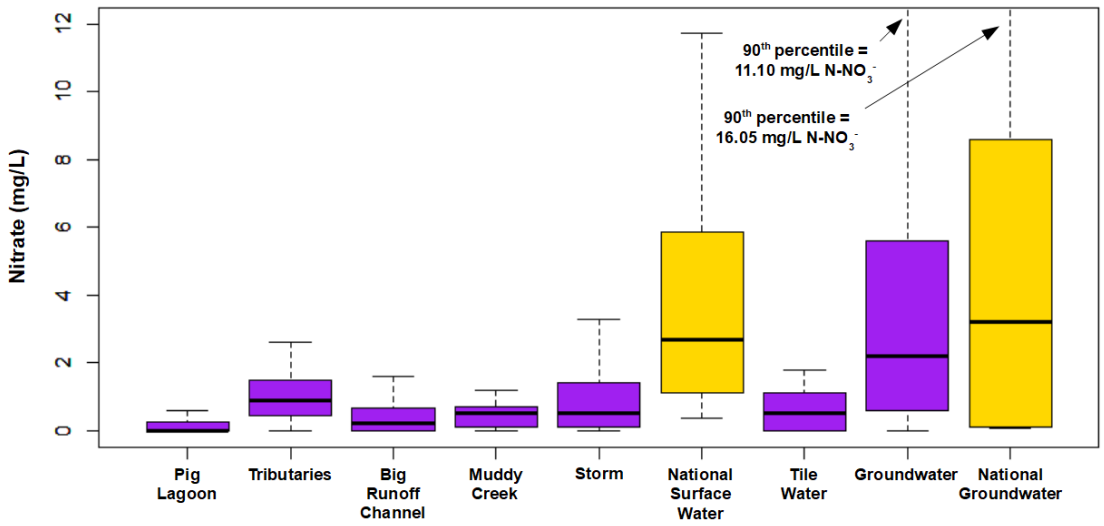


***Figure 12. Box and whisker plots of nitrogen as nitrate ($N\text{-}NO_3^-$) concentrations for different hydrological systems and water types on the Farm compared to national values (Dubrovsky et al., 2010). See Figure 5 for the key.***

***Overall Ammonium Trends***

Overall, Muddy Creek and the pig lagoon have the lowest levels of $NH_4^+$ since they receive minimal contamination from Farm activities. Furthermore, in the pig lagoon and Muddy Creek exhibits lower concentrations national surface water levels (Fig. 13.) However, Farm surface waters exhibit higher concentrations than national values, especially the BRC during storm events, which concurs with previous observations on Farm nutrient chemistry (Buskirk et al., 2017). The highest $NH_4^+$ concentrations on the Farm occur in the cow lagoon (Fig. 7), and these waters are applied across Farm cropland. Storm conditions export lower ammonium concentrations than during baseflow conditions, which suggests dilution during storm conditions.

Groundwater generally exhibits lower ammonium concentrations than Farm surface waters, which concurs with previous observations (Buskirk et al., 2017; Fig. 13). Soil water exhibits similar $NH_4^+$ values to groundwater, which suggests that infiltration of nitrate and subsequent ammonification by bacteria may be a mechanism for increasing ammonium concentrations in soil water and groundwater.

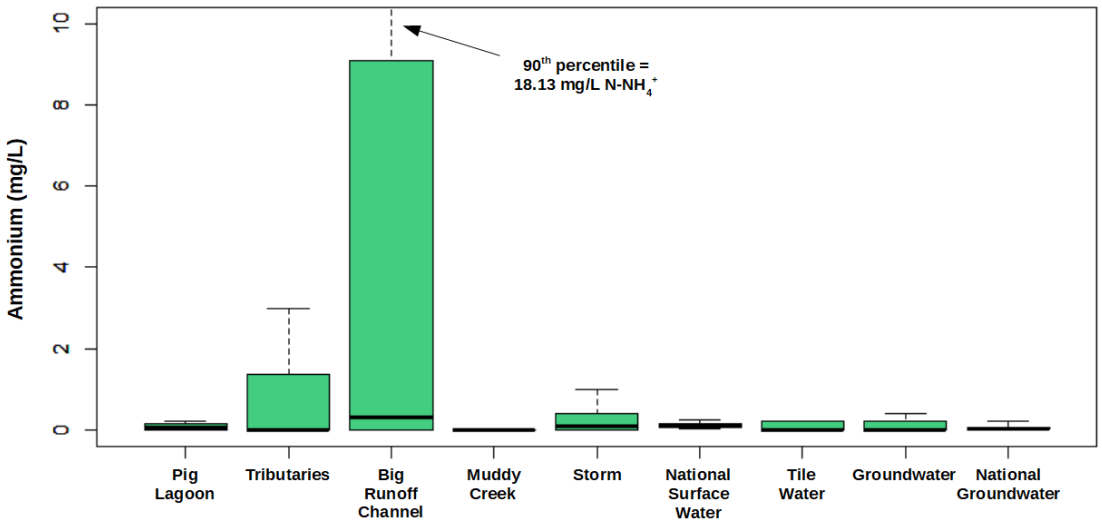


***Figure 13. Box and whisker plots of nitrogen as ammonium (N-$NH_4^+$) concentrations for different hydrological systems and water types on the Farm compared to national values (Dubrovsky et al., 2010). See Figure 5 for the key.***

***Overall Phosphate Trends***

Phosphate concentrations for surface waters (Muddy Creek and Farm tributaries) were significantly lower than national concentrations, which concurs with previous observations (Evans et al., 2017; Fig. 14). However, the BRC and stormwaters were an exception. The BRC and its stormflow exhibit similar median $PO_4^{3-}$ concentrations to national values, but a greater range of high $PO_4^{3-}$ concentrations than national values. This suggests the BRC is a major conduit for nutrient transport during baseflow and storm conditions. The pig lagoon likely exhibits lower $PO_4^{3-}$ concentrations than national values since it is relatively unaffected by Farm activities. Groundwater exhibited similar $PO_4^{3-}$ concentrations to national values.

**Storm Water Chemistry:**

The variations of dissolved major ions during storm water flow points to nutrient transport mechanisms. During the Cindy event, $Ca^{2+}$, $Mg^{2+}$, $Na^{+}$, $Cl^{-}$, $SO_4^{2-}$, and $HCO_3^{-}$ decreased simultaneously from source baseflow concentrations as discharge increased from the BRC (Fig. 15). This behavior represents dilution of groundwater baseflow by precipitation and subsequent overland flow.

However, $K^{+}$ increased from baseflow concentrations, spiking concurrently with increasing BRC discharge, then progressively decreased over the duration of the storm (Fig. 15H). This behavior suggests that $K^{+}$ was immediately flushed from soil. This behavior has been observed at other localities (Ávila et al., 1992). Also, karst conduits may also be a factor.

This initial spike exhibited by $K^{+}$ is also observed for $SO_4^{2-}$, $Cl^{-}$, and $Na^{+}$ at the same time (Fig. 15). This suggests that these compounds are sourced from both groundwater and soil cover during storm events in the same manner as $K^{+}$. Specifically, $SO_4^{2-}$ and $Cl^{-}$ from manure application is likely rapidly washed from the surface during

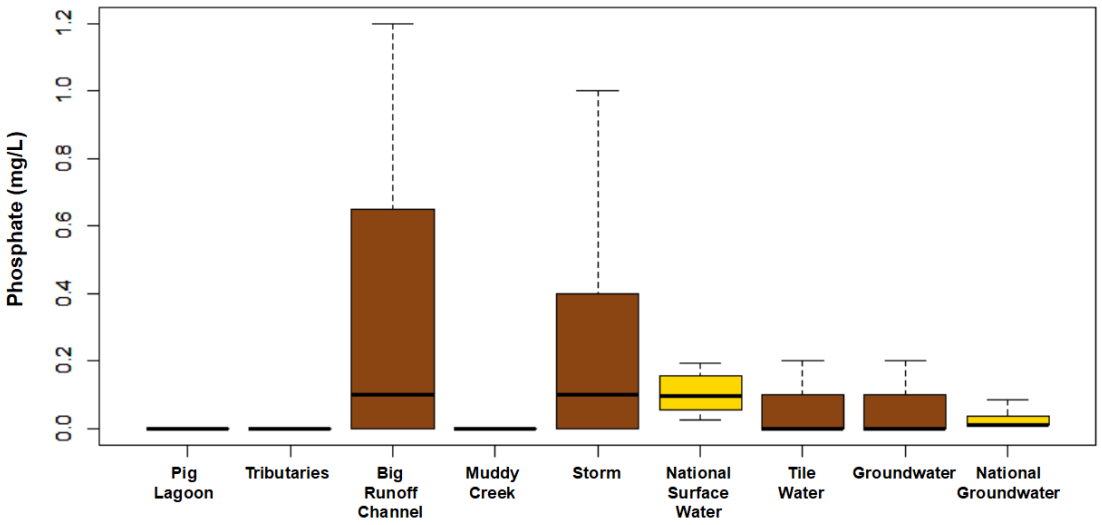


***Figure 14. Box and whisker plots of phosphorus as phosphate ($P\text{-}PO_4^{3-}$) concentrations for different hydrological systems and water bodies on the Farm compared to national values (Dubrovsky et al., 2010). See Figure 5 for the key.***

storm events similarly to $K^+$. However, large $SO_4^{2-}$ and $Cl^-$ concentrations in groundwater from percolation create a constant source of $SO_4^{2-}$ and $Cl^-$, which mimics solutes sourced from bedrock during storms. Local bedrock may be a source for $SO_4^{2-}$ and $Cl^-$. However, the composition of local bedrock requires testing to verify this possibility. Furthermore, $Ca^{2+}$, $Mg^{2+}$, and $HCO_3^-$ are likely sourced almost entirely from local bedrock since they do not exhibit a flushing mechanism.

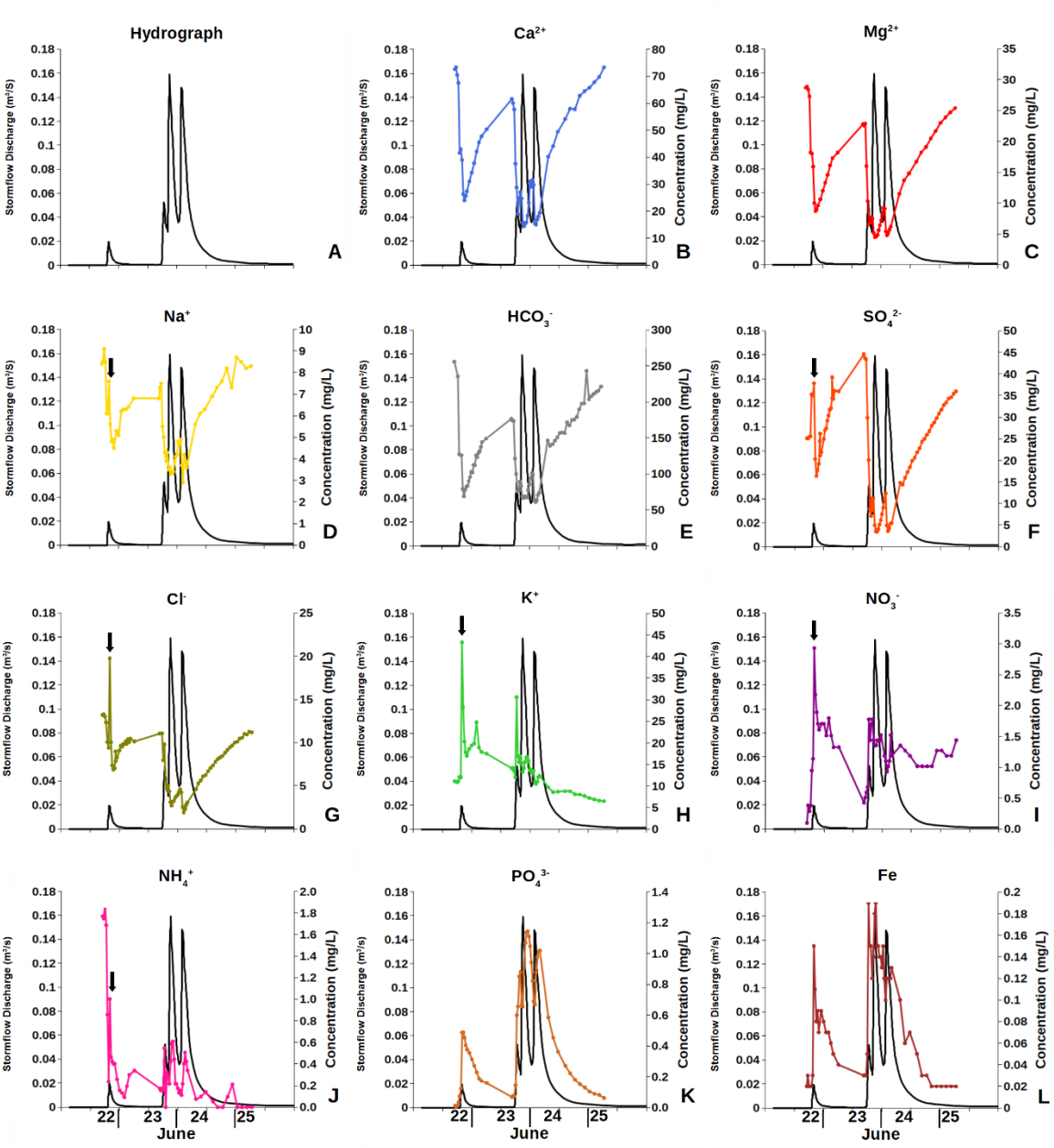


***Figure 15. Hydrographs and dissolved ion concentrations of storm runoff during tropical storm Cindy, June 22-25, 2017. A. Hydrograph of discharge, which concurs with time series concentrations of each ion on subsequent graphs (B through L). The arrows show the simultaneous peaks for discharge on the hydrograph with initial concentration peaks of $Na^+$, $SO_4^{2-}$, $Cl^-$, $K^+$, $NO_3^-$, and $NH_4^+$.***

Nutrient concentrations generally increase with discharge indicating transport by surface runoff. For example, $NO_3^-$ exhibited nearly identical transport behavior as $K^+$; concentration spikes occur simultaneously with $K^+$ and discharge (Fig. 15). However, $NO_3^-$ levels reached higher baseline concentrations during the Cindy event than during pre-storm levels. Also, the initial flushing and prolonged release of $NO_3^-$ in groundwater after the Cindy event suggest retention in soil, groundwater, and/or karst conduits. This concurs with previous studies, since elevated $NO_3^-$ concentrations are observed in groundwater on the Farm. A study of karst conduits is recommended to further constrain $NO_3^-$ behavior, since activation of karst conduits have been observed in the on the Farm.

Background concentration of $NH_4^+$ is generally 0.0 to 0.2 mg/L (Fig. 15). Immediately prior to water flow over the weir during the Cindy event, concentrations were unusually high (~1.7 mg/L). But during the first storm pulse, decreased significantly to <0.04 mg/L. Later in the main storm event, $NH_4^+$ tracked discharge from the weir and afterward returned to typical background concentrations. This behavior suggests rapid release of $NH_4^+$ from soil followed by accumulation within the weir pool and then subsequent flushing during the precipitation event. $NH_4^+$ transport behavior during the main storm event mimics $PO_4^{3-}$ and Fe, which suggests $NH_4^+$ is transported with soil from erosion. This is possible since $NH_4^+$ would be attracted to negatively charged clay surfaces in soils. Furthermore, high $NH_4^+$ levels were observed in the cow lagoon. Therefore, manure application to crops contains a large amount of $NH_4^+$, which could be sorbed to mineral surfaces and then flushed during rainfall events.

$PO_4^{3-}$ concentrations are directly proportional to discharge (Fig 15). Furthermore, Fe mimics $PO_4^{3-}$ behavior, showing that Fe and dissolved $PO_4^{3-}$ are chemically related, likely because P typically binds to Fe in sediments (Lijklema, 1980; Rosenberg & Schroth, 2017; Fig. 15). This suggests that Fe and $PO_4^{3-}$ are proxies for sediment transport.

***Nutrient Sequestration:***

With regards to developing nutrient sequestration techniques, vegetation buffering seems an effective method to reduce erosion to limit $PO_4^{3-}$ and $NH_4^+$ transport. Furthermore, buffering would slow $NO_3^-$ transport, as well. However, $NO_3^-$ export through the local groundwater would not be affected by buffers. Therefore, a more detailed study of local karst conditions is merited.

# Conclusions

(1) Baseflow conditions are dominated by $Ca^{2+}$ - $Mg^{2+}$ - $HCO_3^-$ - rich water sourced from dolomite bedrock.

(2) Baseflow is significantly diluted during storm events by overland flow, which also transports nutrients.

(3) $NO_3^-$ transport mimics that of $K^+$, but shows prolonged release into waters. Further studies are suggested to constrain the role of karst conduits in nutrient transport.

(4) $NH_4^+$ is released by overland flow more rapidly than other nutrients.

(5) $PO_4^{3-}$ and $Fe^{3+}$ track discharge and are likely proxies for sediment transport during storms. This also suggests utilizing vegetation buffers to reduce P export as part of developing sequestration methods.

# References


Ávila, A., Pinol, J., Roda, F., Neal, C., 1992, Storm behavior in a montane Mediterranean forested catchment: Journal of Hydrology, v. 140, p. 143-161.

Actlabs, 2017, CationData_MeadowbrookFarm2017: Activation Laboratories, ID. 08890. (www.actlabs.com)

Buskirk, R.E., Evans, H.R., Borowski, W.S., Malzone, J.M., 2017. Nitrogen in Surface Waters and Groundwater at EKU's Meadowbrook Farm. [Undergraduate Thesis]. Eastern Kentucky University, Richmond Kentucky, May 2017.

Borowski, W.S., Aguiar T.A., Jolly E.C., Hunter J., Stockwell R.D., Albright M.S., Godbey S.E., West B.E. 2012 Characteristics and environmental problems of a eutrophic, seasonally-stratified lake, Wilgreen Lake, Madison County, Kentucky. Journal of the Kentucky Academy Sciences, 73(1):41-69.

Chang, R., Goldsby, K.A., General Chemistry The Essential Concepts, 7th Ed: McGraw-Hill Companies, New York, p. 260.

Clesceri L.S, Greenberg A.E., Eaton A.D., Franson MAH (Eds.), 1998 (20th ed.) Standard Methods for the Examination of Water and Wastewater, APHA, AWWA, WEF. Baltimore: Port City Press.

Dubrovsky N.M., Burow K.R., Clark G.M., Gronberg J.O.M., Hamilton P.A., Hitt, K.J., Mueller D.K., Munn M.D., Nolan B.T., Puckett L.J., Rupert M.G., Short T.M., Spahr N.E., Sprague L.A., Wilber W.G. 2010. The quality of our nation's water – Nutrients in the nation's streams and groundwater, 1992-2004. USGS Circular 1350, 175pp.

Eby, G. Nelson, 2004. Principles of Environmental Geochemistry. Pacific Grove: Brooks Cole.

Evans, H.R., Buskirk, R.E., Borowski, W.S., Malzone, J.M., 2017. Nutrient contamination from non-point sources: Dissolved phosphate in surface and subsurface waters at EKU Meadowbrook Farm, Madison County, Kentucky. [Undergraduate Thesis]. Eastern Kentucky University, Richmond Kentucky, May 2017.

Kelley, L., Borowski, W.S., Malzone, J.M., 2018 Characterization of Groundwater and Surface Water Geochemistry in an Agricultural Setting at EKU's Meadowbrook Farm, Madison County KY [abs.]: Kentucky Water Resources Annual Symposium, Lexington, Kentucky.

Lijklema, L., 1980, Interaction of Orthophosphate with Iron (III) and Aluminum Hydroxides: American Chemical Society, v. 14 (5), p. 537-541.

Kelley, L., H.R. Evans, R.E. Buskirk, J.M. Malzone, and W.S. Borowski. 2017. Groundwater and subsurface water in a landscape with shallow bedrock:

Kentucky Mesonet. Western Kentucky University. http://www.kymesonet.org/live_data.html#!ELST (accessed October 11, 2016).

Gieskes J.M, Gamo T., Brumsack H. 1991. Chemical methods for interstitial water analysis aboard the JOIDES Resolution. *Ocean Drilling Program Technical Note 15*, Ocean Drilling Program, Texas A&M University, 60 pp.

Greene, R.C., 1968. Geologic map of the Moberly Quadrangle, Madison and Estill Counties, Kentucky. Kentucky Geological Survey.

Hach. 1986. Nitrate, Instruction Manual, Pocket Colorimeter II. 73 pp.

Method 4500-$NH_3$ F. Phenate method. *IN* Eaton, A.D., Clesceri L.S., Rice E.W., Greenberg A.E. (Eds.), 2005 (21st ed.). Standard Methods for the Examination of Water and Wastewater. APHA, AWWA, WEF. Baltimore: Port City Press. p. 4-114.

Method 4500-$NO_3$ E. Cadmium reduction method. *IN* Eaton, A.D., Clesceri L.S., Rice E.W., Greenberg A.E. (Eds.), 2005 (21st ed.). Standard Methods for the Examination of Water and Wastewater. APHA, AWWA, WEF. Baltimore: Port City Press. pp. 4-123 to 4-125.

Rosenberg, B.D.; Schroth, A.W., 2017, Coupling of reactive riverine phosphorus and iron species during hot transport moments: impacts of land cover and seasonality: Biogeochemistry, v. 132, p. 103-122.

Strickland JDH, Parsons TR. 1968. A manual for sea water analysis. Bull. Fisheries Research Board Canada, 167: 49-55. Gieskes JM, Gamo T, Brumsack H, 1991. Phosphate. *In:* Chemical methods for interstitial water analysis aboard the JOIDES Resolution. *Ocean Drilling Program Technical Note 15*, Ocean Drilling Program, Texas A&M University, pp. 46-47, 60.

Solorzano L. 1969. Determination of ammonia in natural waters by phenol-hypochlorite method. *Limnology Oceanography*. 14:799-801.

# Appendix

## Table A1. GPS coordinates of Farm sampling sites.

| | | NORTH LATITUDE | | | WEST LONGITUDE | | |
|---|---|---|---|---|---|---|---|
| | **Site** | **Degrees** | **Minutes** | **Seconds** | **Degrees** | **Minutes** | **Seconds** |
| **Springs** | Spring 1 | 37 | 42 | 59.736 | -84 | 9 | 13.164 |
| | Spring 2 | 37 | 43 | 9.126 | -84 | 8 | 56.429 |
| | Spring 2B | 37 | 43 | 7.864 | -84 | 8 | 55.211 |
| | Spring 3 | 37 | 43 | 9.349 | -84 | 8 | 52.255 |
| | Spring 4 | 37 | 43 | 9.284 | -84 | 8 | 50.910 |
| | Spring 5 | 37 | 43 | 10.995 | -84 | 8 | 38.553 |
| | Spring 6 | 37 | 43 | 28.487 | -84 | 8 | 54.910 |
| | Spring 7 | 37 | 43 | 8.505 | -84 | 8 | 58.903 |
| | Spring 8 | 37 | 43 | 9.040 | -84 | 9 | 7.555 |
| | Spring 9 | 37 | 43 | 14.747 | -84 | 9 | 9.281 |
| | Spring 10 | 37 | 43 | 7.903 | -84 | 9 | 10.192 |
| **Surface** | Steel bridge | 37 | 42 | 38.355 | -84 | 9 | 37.900 |
| | MR C | 37 | 43 | 23.718 | -84 | 9 | 46.797 |
| | MR culvert | 37 | 42 | 55.457 | -84 | 9 | 30.885 |
| | trib 0 W | 37 | 42 | 46.349 | -84 | 9 | 26.313 |
| | trib 1 E | 37 | 42 | 47.129 | -84 | 9 | 13.138 |
| | trib 2 W | 37 | 42 | 59.890 | -84 | 9 | 11.650 |
| | trib 3 E | 37 | 43 | 3.554 | -84 | 9 | 5.603 |
| | trib 5 W | 37 | 43 | 4.948 | -84 | 9 | 6.236 |
| | trib 5W-d | 37 | 43 | 5.499 | -84 | 9 | 2.517 |
| | trib 6 E | 37 | 43 | 3.994 | -84 | 8 | 57.405 |
| | trib 7 W | 37 | 43 | 7.755 | -84 | 8 | 52.581 |
| | trib 8 W | 37 | 43 | 10.735 | -84 | 8 | 38.019 |
| | trib 9E | 37 | 43 | 12.049 | -84 | 8 | 36.165 |
| | trib 10 E | 37 | 43 | 22.453 | -84 | 8 | 35.866 |
| | trib 10d W | 37 | 43 | 27.181 | -84 | 8 | 43.314 |
| | trib 11 W | 37 | 43 | 27.594 | -84 | 8 | 45.532 |
| | trib 12 W | 37 | 43 | 29.485 | -84 | 8 | 47.649 |
| | trib 13 E | 37 | 43 | 32.537 | -84 | 9 | 28.761 |
| | trib 14 E | 37 | 43 | 46.541 | -84 | 9 | 30.957 |
| | trib 15 W | 37 | 43 | 39.309 | -84 | 8 | 49.294 |
| | trib 16 W | 37 | 43 | 42.711 | -84 | 8 | 53.661 |
| | XSF | 37 | 43 | 43.587 | -84 | 8 | 54.010 |
| **Tile drains** | Tile 0 | 37 | 42 | 39.618 | -84 | 9 | 38.661 |
| | Tile 1 | 37 | 42 | 45.661 | -84 | 9 | 26.486 |
| | Tile 2 | 37 | 42 | 47.848 | -84 | 9 | 25.242 |
| | Tile 3 | 37 | 42 | 48.187 | -84 | 9 | 24.375 |
| | Tile 4 | 37 | 42 | 48.724 | -84 | 9 | 23.937 |
| | Tile 5 | 37 | 42 | 55.383 | -84 | 9 | 11.301 |
| **Big Runoff Channel Baseline** | North Branch | 37 | 43 | 7.888 | -84 | 9 | 7.999 |
| | North Branch Outlet | 37 | 43 | 14.286 | -84 | 9 | 7.409 |
| | Central Branch | 37 | 43 | 11.197 | -84 | 9 | 9.021 |
| | South Branch Outlet | 37 | 43 | 9.517 | -84 | 9 | 18.608 |
| | South Branch corn | 37 | 43 | 9.319 | -84 | 9 | 19.256 |

| | | | | | | |
|---|---|---|---|---|---|---|
| Big runoff channel | 37 | 43 | 6.068 | -84 | 9 | 7.343 |
| BRC | 37 | 43 | 6.303 | -84 | 9 | 7.489 |
| BRC Tile | 37 | 43 | 12.151 | -84 | 9 | 7.878 |
| W1 | 37 | 43 | 6.198 | -84 | 9 | 6.553 |
| A | 37 | 43 | 21.682 | -84 | 9 | 7.797 |
| B | 37 | 43 | 29.095 | -84 | 9 | 14.268 |
| C | 37 | 43 | 17.221 | -84 | 9 | 16.341 |
| D | 37 | 43 | 9.524 | -84 | 9 | 19.827 |
| E | 37 | 43 | 9.458 | -84 | 9 | 18.598 |
| F | 37 | 43 | 8.782 | -84 | 9 | 17.544 |
| G | 37 | 43 | 9.477 | -84 | 9 | 11.329 |
| H | 37 | 43 | 7.777 | -84 | 9 | 13.436 |
| I | 37 | 43 | 8.065 | -84 | 9 | 10.607 |
| J | 37 | 43 | 9.275 | -84 | 9 | 9.515 |
| K | 37 | 43 | 7.748 | -84 | 9 | 9.557 |
| M | 37 | 43 | 8.194 | -84 | 9 | 7.907 |
| N | 37 | 43 | 6.895 | -84 | 9 | 7.834 |
| O | 37 | 43 | 7.171 | -84 | 9 | 8.518 |
| P | 37 | 43 | 7.364 | -84 | 9 | 8.429 |
| Q | 37 | 43 | 7.340 | -84 | 9 | 8.797 |
| R | 37 | 43 | 8.334 | -84 | 9 | 11.005 |
| S | 37 | 43 | 8.179 | -84 | 9 | 11.297 |
| T | 37 | 43 | 8.407 | -84 | 9 | 9.981 |
| U | 37 | 43 | 8.108 | -84 | 9 | 12.402 |
| V | 37 | 43 | 8.252 | -84 | 9 | 14.316 |
| X | 37 | 43 | 8.234 | -84 | 9 | 16.236 |
| Y | 37 | 43 | 9.067 | -84 | 9 | 18.531 |
| Z | 37 | 43 | 10.551 | -84 | 9 | 18.189 |
| Rx | 37 | 43 | 11.963 | -84 | 9 | 17.563 |
| Rz | 37 | 43 | 9.492 | -84 | 9 | 7.898 |

**Figure A2. Typical nutrient calibration plots used to determine $N\text{-}NO_3^-$ (a), $N\text{-}NH_4^+$ (b), and $P\text{-}PO_4^{3-}$ (c) concentrations.**

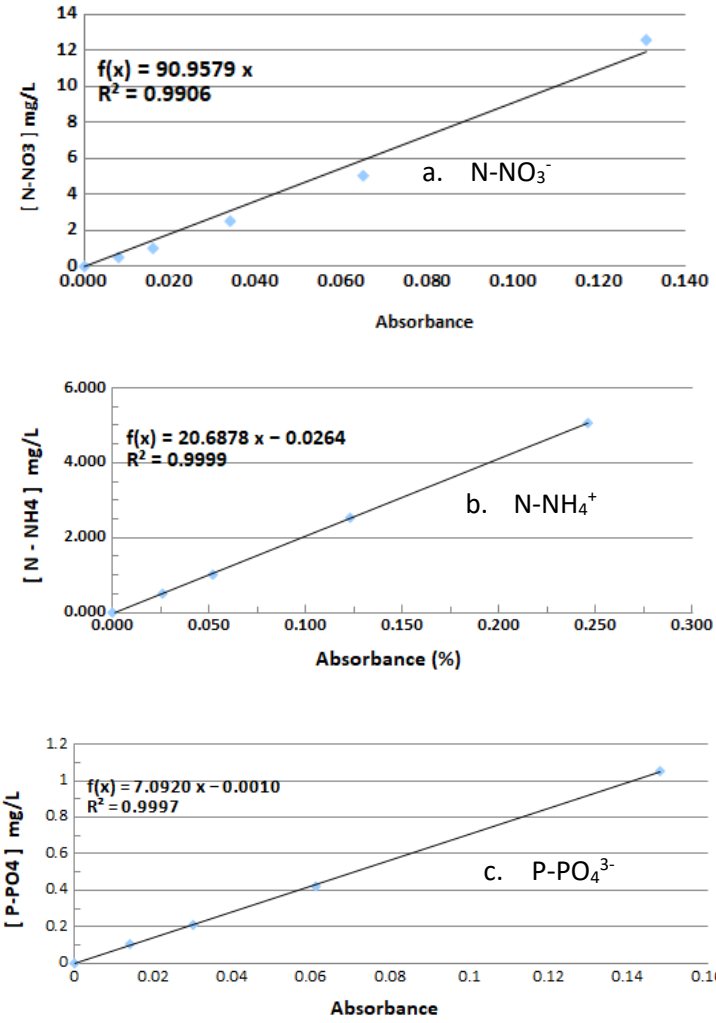

**Table A3. Tabulated $r^2$ values for nutrient calibration curves.**

| $r^2$ values generated from nutrient calibration plots | | |
|---|---|---|
| Nitrate | Ammonium | Phosphate |
| 0.987 | 0.9997 | 0.9999 |
| 0.9934 | 0.9997 | 0.9994 |
| 0.9899 | 0.9999 | 0.9991 |
| 0.999 | 0.9986 | 0.9994 |
| 0.9904 | 0.9978 | 0.9997 |
| 0.9995 | 0.9896 | 0.9998 |
| 0.9955 | 0.9988 | 0.9998 |
| 0.9941 | 0.9991 | 0.9998 |
| 0.9929 | 0.9844 | 0.9998 |
| 0.9941 | 0.997 | 0.9997 |
| 0.9974 | 0.9961 | 0.9987 |
| 0.9966 | 0.9997 | 0.999 |
| 0.9863 | 0.9907 | 0.9999 |
| 0.9979 | 0.9895 | 0.9999 |
| - | 0.9944 | 0.9999 |
| - | 0.9866 | 0.9997 |

**Figures A4. Example of anion calibration plots from IC measurements.**

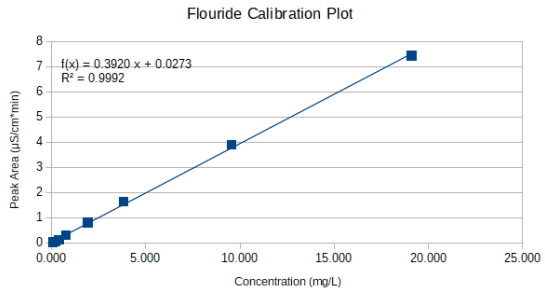


***a. Example fluoride calibration plot***

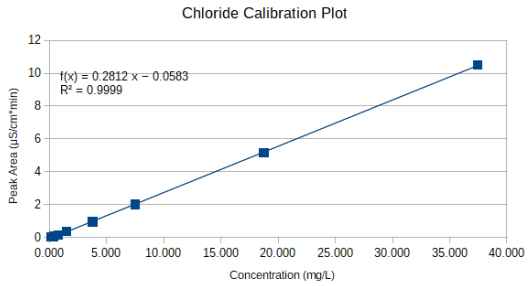


***b. Example chloride calibration plot***

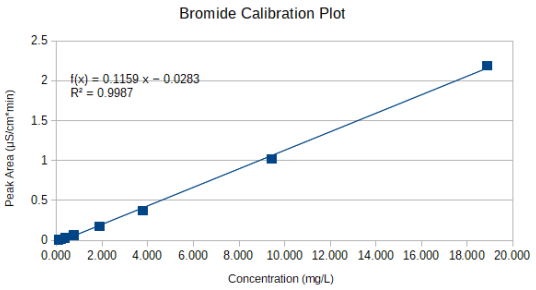


***c. Example bromide calibration plot***

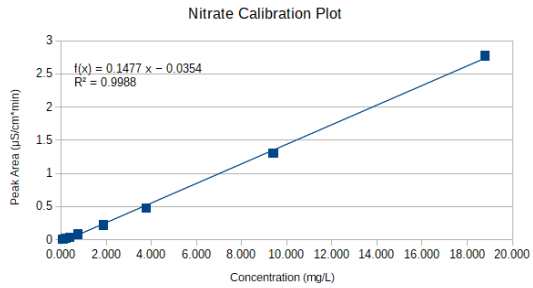


***d. Example nitrate calibration plot***

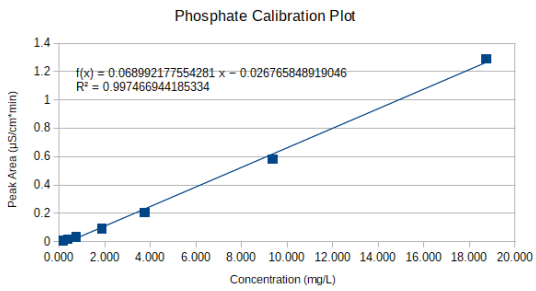


***e. Example phosphate calibration plot***

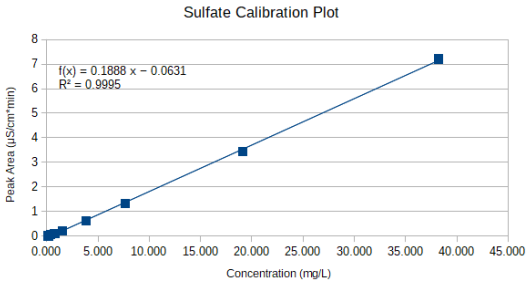


***f. Example sulfate calibration plot***

**Table A5. Tabulated $r^2$ values from calibration curves for fluoride, chloride, bromide, nitrate, phosphate, and sulfate.**

| $r^2$ values generated from anion calibration plots | | | | | |
|---|---|---|---|---|---|
| Fluoride | Chloride | Bromide | Nitrate | Phosphate | Sulfate |
| 0.9990 | 1.0000 | 0.9991 | 0.9987 | 0.9972 | 0.9997 |
| 0.9988 | 1.0000 | 0.9992 | 0.9992 | 0.9979 | 0.9997 |
| 0.9992 | 0.9999 | 0.9988 | 0.9989 | 0.9972 | 0.9993 |
| 0.9992 | 0.9999 | 0.9987 | 0.9988 | 0.9975 | 0.9995 |
| 0.9994 | 0.9998 | 0.9996 | 0.9997 | 0.9983 | 0.9998 |
| 1.0000 | 1.0000 | 0.9995 | 0.9996 | 0.9977 | 0.9999 |
| 0.9990 | 1.0000 | 0.9993 | 0.9993 | 0.9975 | 0.9997 |
| 0.9990 | 1.0000 | 0.9991 | 0.9987 | 0.9972 | 0.9997 |
| 0.9991 | 1.0000 | 0.9993 | 0.9985 | 0.9980 | 0.9998 |

**Table A6.** Tabulated percent difference calculations for duplicates.

| | $F^-$ | | $Cl^-$ | | $Br^-$ | | $NO_3^-$ | | $PO_4^{3-}$ | | $SO_4^{2-}$ | |
|---|---|---|---|---|---|---|---|---|---|---|---|---|
| Sample ID | [mg/L] | % Difference | [mg/L] | % Difference | [mg/L] | % Difference | [mg/L] | % Difference | [mg/L] | % Difference | [mg/L] | % Difference |
| W1 8/4/17-16:44-Duplicate | 0.029 | 6.5 | 24.276 | 0.1 | 0.260 | 0.0 | 4.408 | 0.2 | 1.000 | 0.4 | 32.941 | 0.3 |
| W1 8/4/17-16:44 | 0.033 | | 24.342 | | 0.260 | | 4.423 | | 1.008 | | 33.113 | |
| W1 8/4/17-14:14-Duplicate | 0.043 | 2.4 | 29.452 | 0.4 | 0.264 | 0.2 | 4.922 | 1.0 | 1.153 | 0.3 | 38.005 | 0.3 |
| W1 8/4/17-14:14 | 0.041 | | 29.201 | | 0.265 | | 4.827 | | 1.145 | | 37.804 | |
| W1 5/5/17-1:04-Duplicate | 0.000 | - | 4.191 | 1.4 | | - | 2.017 | 4.0 | 1.186 | 0.0 | 20.846 | 0.3 |
| W1 5/5/17-1:04 | 0.000 | | 4.078 | | | | 1.861 | | 1.187 | | 20.971 | |
| W1 5/4/17-21:34-Duplicate | 0.000 | 100.0 | 8.516 | 1.0 | | - | 0.328 | 0.0 | | - | 50.005 | 0.9 |
| W1 5/4/17-21:34 | 0.021 | | 8.682 | | | | 0.328 | | | | 49.093 | |
| W1 6/24/17-3:01-Duplicate | 0.000 | - | 2.398 | 2.3 | | - | 1.583 | 0.9 | 2.173 | 0.8 | 4.172 | 2.9 |
| W1 6/24/17-3:01 | 0.000 | | 2.509 | | | | 1.611 | | 2.206 | | 4.419 | |
| W1 6/23/17-19:31-Duplicate | 0.000 | - | 4.985 | - | | - | | - | 1.874 | 34.0 | | - |
| W1 6/23/17-19:31 | 0.000 | | 4.857 | | | | | | 0.924 | | | |